Journal of Simulation and Analysis of Novel Technologies in Mechanical Engineering
14 (1) (2022) 0005~0018
HTTP://JSME.IAUKHSH.AC.IR

Research article

Frequency responses analysis of clamped-free sandwich beams with porous FG face sheets

Mohsen Rahmani*

Department of Mechanics, Tuyserkan Branch, Islamic Azad University, Tuyserkan, Iran

*Mohsen_rahmani@ymail.com

(Manuscript Received --- 04 Jan. 2022; Revised --- 21 Jan. 2022; Accepted --- 04 Feb. 2022)

Abstract

In this paper, the frequency responses analysis of the sandwich beams with functionally graded face sheets and homogeneous core is investigated based on the high order sandwich beam theory. All materials are temperature dependent and the functionally graded materials properties are varied gradually by a power law rule which is modified by considering the even and uneven porosity distributions. The nonlinear Lagrange strain and the thermal stresses of the face sheets and in-plane strain and transverse flexibility of the core are considered. Hamilton's principle and Galerkin method are used to obtain and solve the equations for the clamped-free boundary condition. To verify the results of this study, they compared with special cases of the literatures. Based on the numerical results, it is concluded that by increasing the temperature, power law index, length, thickness, porosity volume fraction the fundamental frequency parameter decreases and increasing the wave number causes the frequency increases.

Keywords: Sandwich beam, FGM, Porosity, Temperature dependent, Clamped-free.

1- Introduction

Nowadays, the sandwich panels which usually have two thin and stiff faces and a lightweight flexible core have become the common and useful structures in the modern industries such as aerospace, transportation, naval and construction structures. These structures have a high bending rigidity, high performance with a low weight concurrently [1].

On the other hand, the failure, delamination and the thermal stress concentration are the results of using the classical composite materials in the high temperature environments. To avoid these damages, the functionally graded materials (FGMs) have been proposed which are microscopic inhomogeneous materials and gradually graded from a metal surface to a ceramic one [2].

In the classical theories, the core has been considered as a constant thickness layer, but to investigate the localized effects in the sandwich structures behavior, the high order sandwich panels theory is presented and the core is considered as a transversely flexible layer [3]. Many researchers have been studied the mechanical behaviors of

sandwich beams by using different theories. Fazzolari studied the vibration and elastic stability of functionally graded sandwich beams resting on the elastic foundation by using a higher beam theory [4]. Based on the Timoshenko beam theory, Chen et al. studied the nonlinear vibration of sandwich beam with porous FG core and solved the equation by applying Ritz method theory [5]. Akbaş investigated the vibration of FG porous deep beam based on a finite element procedure under the thermal conditions [6]. Bourada et al. studied the vibration of FG beams with porosity based on a high order trigonometric deformation theory [7]. Li et al. studied the nonlinear vibration of FG sandwich beams with negative Poisson's ratio honeycomb core based on the 3D full-scale finite element analyses [8]. Wu et al. surveyed the vibration and buckling of sandwich beams with FG carbon nanotube-reinforced composite faces based on the Timoshenko beam theory [9]. Xu et al. investigated the vibration of composite sandwich beam with corrugated core based on the continuous homogeneous theory and Rayleigh-Ritz method [10]. Li et al. investigated the vibration of multilayer lattice sandwich beams numerically and experimentally [11]. Li investigated the nonlinear vibration and stability of axially moving viscoelastic sandwich beam under resonances by using Galerkin method [12]. Şimşek and Al-shujairi investigated different types of vibration behaviors of FG sandwich beams under the harmonic loads by using Timoshenko beam theory [13]. Nguyen et al. studied the buckling and vibration behaviors of different types of FG sandwich beams by using a quasi 3D beam theory [14]. By using a finite element model, Kahya and Turan investigated the buckling and vibration of different types of FG sandwich beams based on the first order shear deformation theory [15]. Tossapanon and Wattanasakulpong studied the buckling and vibration behavior of sandwich beams with FG faces resting on elastic foundation based on the Timoshenko beam theory and Chebyshev collocation [16]. Arikoglu and Ozkol investigated the vibration of composite sandwich beams with viscoelastic core based on differential transform method [17]. Pradhan and Murmu investigated the vibration of FG beams and FG sandwich beams resting on elastic foundations by using differential quadrature method [18]. Mashat et al. studied the vibration of FG layered beams by using Carrera unified formulation and FEM [19]. Nguyen et al. studied the vibration and buckling of FG sandwich beams based on the higher order shear deformation theory [20]. Vo et al. studied the vibration and buckling of FG sandwich beams by using a quasi 3D theory and a finite element model [21]. Yang et al. studied the vibration behavior of the different type of the FG sandwich beams by using a meshfree boundary-domain integral equation method [22]. Abdolahi and Yas Studied the vibration of Timoshenko beam with the elastic foundation by using Timoshenko theory [23]. Farahani et al. studied the vibration behavior of thick FG beam under axial load based on the elasticity theory [24]. Pirmoradian and Karimpour studied the dynamic stability of a beam which excited by transition of circulating masses by considering the effects of convective mass acceleration and large deformation beam theory [25]. Pirmoradian et al. investigated the instability of double walled carbon nanotubes surrounded by elastic medium based on the Euler-Bernoulli beams model

and a nonlocal elastic theory [26],[27]. Torkan et al. studied transverse vibration of a rectangular plate on an elastic foundation and the instability due to occurrence of parametric resonance under passage of continuous series of moving masses [28]. Torkan et al. studied the dynamic stability of the thick rectangular plate carrying an orbiting mass and lying on a viscoelastic foundation based on the first order shear deformation theory [29]. Torkan and Pirmoradian studied the daynamic stability of thick elastic plates carrying a moving mass based on different higher order shear deformation theory [30]. Heydari et al. studied the sound transmission loss of porous heterogeneous cylindrical nanoshell based on a nonlocal strain gradient and first order shear deformation theories [31]. Heydari et al. studied the acoustic wave transmission of double walled FG cylindrical microshell in thermal conditions based on a modified strain gradient theory [32].

After studying the accessible references, it is concluded that more studying about the beam mechanical behavior is needed. Also, analyzing the temperature dependent vibration behavior of sandwich beams with porous functionally graded materials skins and considering the flexibility and lateral displacement of the core for clamped-free boundary condition has not been reported. So, in this study, by applying a high order sandwich beam theory which modified by considering the flexibility of the core in the thickness direction, frequency responses of the sandwich beams is investigated. Sandwiches consist of two FG faces which cover a homogeneous core. All materials are temperature dependent and FGM properties are location dependent which graded in according to a power law rule. To increase the accuracy of the model of the FGM properties, even and uneven porosity distributions are applied. Nonlinear Lagrange strain and thermal stresses of the face sheets and in-plane strain of the core are considered. Governing equations of the motion are obtained based on the Hamilton's principle and solved by a Galerkin method for the clamped-free boundary condition. In order to validate the present approach, special cases of the results of this analytical approach are compared with some literatures. Finally, the effects of the temperature, power law index, some geometrical parameters and porosity on the vibration characteristics of the defined sandwich beams are investigated.

2-Formulation

Consider a sandwich beam with two FG face-sheets and a homogeneous core with a clamped-free boundary condition as shown in Fig. 1.

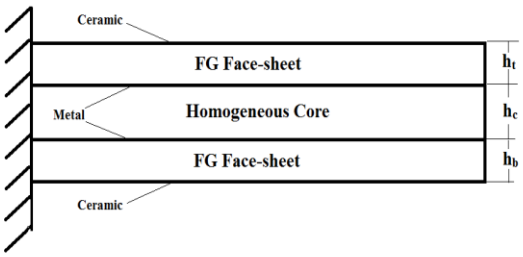

Fig. 1 A schematic of clamped-free FG sandwich beam

The properties of the homogeneous and the FG materials are temperature dependent which defined as follows [33]:

$$P = P_0\left(P_{-1}T^{-1} + 1 + P_1T + P_2T^2 + P_3T^3\right) \qquad (1)$$

where "P"s are coefficients of temperature, and they are unique for each material; $T=T_0+\Delta T$, which T_0 is equal to 300(K). Usually, it is considered that functionally graded materials are composed of metal and ceramic. Material properties such as

Young's modulus, density, Poisson's ratio are varied gradually across the thickness direction. The power law rule which consists of even porosity distribution is presented as follow [34]:

$$P_j\left(z_j,T\right)=g\left(z_j\right)P_{ce}^{j}\left(T\right)+\left[1-g\left(z_j\right)\right]P_m^{j}\left(T\right) -(P_{ce}^{j}\left(T\right)+P_m^{j}\left(T\right))\frac{\zeta}{2} \quad (2)$$

$$g\left(z_t\right)=(\frac{\frac{h_t}{2}-z_t}{h_t})^N;\ \ g\left(z_b\right)=(\frac{\frac{h_b}{2}+z_b}{h_b})^N; \quad j=(t,b) \quad (3)$$

where "N" is the constant power law index; $g(z)$ and $[1\text{-}g(z)]$ are volume fraction of ceramic and metal; "ζ" is the porosity distribution; subscripts "*m*" and "*ce*" refer to metal and ceramic; and subscripts "*t*" and "*b*" refer to top and bottom face sheets, respectively. In the uneven case, the micro voids are spread in the middle area of the layers and decrease near to the edges and tend to the zero. So, power law rule in the uneven case is modified as follows [34]:

$$P_j\left(z_j,T\right)=g\left(z_j\right)P_{ce}^{j}\left(T\right)+\left[1-g\left(z_j\right)\right]P_m^{j}\left(T\right) -(P_{ce}^{j}\left(T\right)+P_m^{j}\left(T\right))\frac{\zeta}{2}(1-\frac{2\left|z_j\right|}{h}),\ (j=t,b) \quad (4)$$

To model the displacement fields of the face-sheets, First Order Shear Deformation Theory (FSDT) is employed as follows [35]:

$$u_j\left(x,z,t\right)=u_{0j}\left(x,t\right)+z_j\phi_j;\ \ j=(t,b) \quad (5)$$

$$w_j\left(x,z,t\right)=w_{0j}\left(x,t\right) \quad (6)$$

where "0" denotes values with correspondence to the central plane of the layers. "*u*" and "*w*" are the in-plane deformation and the transverse deflections of the faces in the "*x*" and "*z*" directions, respectively. "Φ" is the rotation of transvers normal line. Also, the kinematic relations of the core are considered as polynomial pattern with the unknown coefficients, u_k (k=0,1,2,3), for the in-plane and w_l (l=0,1,2) for vertical displacement components which obtained by the variational principle [36]:

$$u_c\left(x,z_c,t\right)=u_0\left(x,t\right)+u_1\left(x,t\right)z_c+u_2\left(x,t\right)z_c^{2} +u_3\left(x,t\right)z_c^{3} \quad (7)$$

$$w_c\left(x,z_c,t\right)=w_0\left(x,t\right)+w_1\left(x,t\right)z_c +w_2\left(x,t\right)z_c^{2} \quad (8)$$

In this theory, the compatibility conditions assume that the faces are sticked to the core completely. The displacements of the interface between the core and the face sheets can be obtained as follows [37]:

$$u_c\left(z_c=-h_c/2\right)=u_t\left(z_t=h_t/2\right), \quad (9)$$

$$w_c\left(z_c=-h_c/2\right)=w_t$$

$$u_b\left(z_b=-h_b/2\right)=u_c\left(z_c=h_c/2\right), \quad (10)$$

$$w_b=w_c\left(z_c=h_c/2\right)$$

To obtain the governing equations of the motion, Hamilton's energy principle is applied as follow:

$$\int_{t1}^{t2}(-\delta K+\delta U)dt=0 \quad (11)$$

The variation of the kinetic and the strain energy are "δK" and "δU", respectively; "*t*" is the time coordinate that varies between the times "t_1" and "t_2"; "δ" is the variation operator. The variation of the kinetic energy is calculated as follows:

$$\begin{aligned}&\int_{t1}^{t2}\delta K dt = \\ &-\int_{t1}^{t2}\{\int_{0}^{L}\int_{-\frac{h_t}{2}}^{\frac{h_t}{2}}\rho_t\left(z_t\right)(\ddot{u}_t\delta u_t+\ddot{w}_t\delta w_t)dxdz_t \\ &+\int_{0}^{L}\int_{-\frac{h_b}{2}}^{\frac{h_b}{2}}\rho_b\left(z_b\right)(\ddot{u}_b\delta u_b+\ddot{w}_b\delta w_b)dxdz_b \\ &+\int_{0}^{L}\int_{-\frac{h_c}{2}}^{\frac{h_c}{2}}\rho_c(\ddot{u}_c\delta u_c+\ddot{w}_c\delta w_c)dxdz_c\}dt\end{aligned} \tag{12}$$

where (··) indicates the second derivative with respect to time; the density is "ρ" which in the functionally graded layers is the function of the displacement; the core is indicated with "*c*". The variation of the total strain energy in the face sheets and the core, also the compatibility conditions at the interfaces of the layers which are the constraints and attended in the Hamilton's principle in terms of Lagrange multipliers, is expressed as follows:

$$\begin{aligned}&\delta U_p=\int_{A_t}(\sigma^t_{xx}\delta\varepsilon^t_{xx}+\sigma^{tT}_{xx}\delta d^t_{xx}+\tau^t_{xz}\delta\gamma^t_{xz}+\sigma^{tT}_{zz}\delta d^t_{zz})dA+\\ &\int_{A_b}(\sigma^b_{xx}\delta\varepsilon^b_{xx}+\sigma^{bT}_{xx}\delta d^b_{xx}+\tau^b_{xz}\delta\gamma^b_{xz}+\sigma^{bT}_{zz}\delta d^b_{zz})dA+\\ &\int_{A_{core}}(\sigma^c_{xx}\delta\varepsilon^c_{xx}+\sigma^c_{zz}\delta\varepsilon^c_{zz}+\tau^c_{xz}\delta\gamma^c_{xz})dA+\\ &\delta\int_0^L[\lambda_{xt}\left(\mathrm{u_t}\left(z_t=\frac{h_t}{2}\right)-u_c\left(z_c=-\frac{h_c}{2}\right)\right)+\\ &\lambda_{zt}\left(\mathrm{w_t}-\mathrm{w_c}\left(z_c=-\frac{h_c}{2}\right)\right)+\\ &\lambda_{xb}(\mathrm{u_c}\left(z_c=\frac{h_c}{2}\right)-u_b\left(z_b=-\frac{h_b}{2}\right)+\\ &\lambda_{zb}\left(\mathrm{w_c}\left(z_c=\frac{h_c}{2}\right)-w_b\right)]dx\end{aligned} \tag{13}$$

where "σ_{xx}" is the in-plane normal stress; "τ_{xz}" is the in-plane shear stresses; "ε_{xx}" and "γ_{xz}" display the in-plane normal and shear linear strains; "d_{xx}" and "d_{zz}" are the in-plane normal and shear nonlinear strains of the layers; "σ^T_{xx}" and "σ^T_{zz}" express the thermal stresses; "σ^c_{zz}" and "ε^c_{zz}" present the lateral normal stress and strain in the core; "τ^c_{xz}" and "γ^c_{xz}" declare shear stresse and shear strain in the core; and "λ_x' and "λ_z" are the Lagrange multipliers.

By considering small deflection, the strain components for the faces can be declared as follows [38]:

$$\varepsilon^j_{xx}=u_{j,x},\ j=(t,b) \tag{14}$$

$$d^j_{xx}=+\frac{1}{2}\left(w_{j,x}\right)^2-\alpha_j\Delta T_j \tag{15}$$

$$\gamma^j_{xz}\left(x,z_j,t\right)=\phi_j(x,t)+w_{j0,x}(x,t) \tag{16}$$

$$d^j_{zz}=\frac{1}{2}\phi^2_{jx}-\alpha_j\Delta T_j \tag{17}$$

The "(),i" expresses the derivation with respect to "i". The strain of the core can be defined as [38]:

$$\varepsilon^c_{xx}\left(x,z_c,t\right)=u_{c,x}\left(x,z_c,t\right) \tag{18}$$

$$\begin{aligned}&\gamma^c_{xz}\left(x,z_c,t\right)=u_{c,z}\left(x,z_c,t\right)+\\ &w_{c,x}\left(x,z_c,t\right)\end{aligned} \tag{19}$$

$$\varepsilon^c_{zz}\left(x,z_c,t\right)=w_{c,z}\left(x,z_c,t\right) \tag{20}$$

In this model by substituting the expressions of the Eq. (12) and Eq. (13) according to the kinematic relations of the layers and using the interfaces relations, and after some algebraic operations, the thirteen equations of motion are obtained. These equations are not independent and by using the compatibility conditions and based on a reduction method the number of equations are reduced to nine. These equations include two unknowns of the faces and seven unknowns of the core which are presented in the follows:

$$\begin{aligned}&+I_{0t}\ddot{u}_{0c}\,h_t/2-I_{1t}\ddot{u}_{0c}-I_{0t}\ddot{\phi}_{0c}\,h_t h_c/4\\ &+I_{1t}\ddot{\phi}_{0c}\,h_c/2+I_{0t}\ddot{u}_{2c}\,h_t h_c^2/8\\ &-I_{1t}\ddot{u}_{2c}\,h_c^2/4-I_{0t}\ddot{u}_{3c}\,h_t h_c^3/16+\\ &I_{1t}\ddot{u}_{3c}\,h_c^3/8-I_{0t}\ddot{\phi}_t\,h_t^2/4+I_{1t}\ddot{\phi}_t h_t\\ &-I_{2t}\ddot{\phi}_t+h_t/2N^t_{xx,x}-M^t_{xx,x}+\\ &N^t_{xz}+N^{tT}_{zz}\phi_t=0\end{aligned} \tag{21}$$

$$
\begin{aligned}
&-I_{0b}\ddot{u}_{0c}\,h_b/2-I_{1b}\ddot{u}_{0c}-I_{0b}\ddot{\phi}_{0c}\,h_b h_c/4\\
&-I_{1b}\ddot{\phi}_{0c}\,h_c/2-I_{0b}\ddot{u}_{2c}\,h_b h_c^2/8-\\
&I_{1b}\ddot{u}_{2c}\,h_c^2/4-I_{0b}\ddot{u}_{3c}\,h_b h_c^3/16-\\
&I_{1b}\ddot{u}_{3c}\,h_c^3/8-I_{0b}\ddot{\phi}_b\,h_b^2/4-I_{1b}\ddot{\phi}_b h_b-I_{2b}\ddot{\phi}_b-\\
&h_b/2N^{b}_{xx,x}-M^{b}_{xx,x}+N^{b}_{xz}+N^{bT}_{zz}\phi_b=0
\end{aligned}
\tag{22}
$$

$$
\begin{aligned}
&-I_{0t}\ddot{u}_{0c}+I_{0t}\ddot{\phi}_{0c}\,h_c/2-I_{0t}\ddot{u}_{2c}\,h_c^2/4+\\
&I_{0t}\ddot{u}_{3c}\,h_c^3/8+I_{0t}\ddot{\phi}_t\,h_t/2-I_{1t}\ddot{\phi}_t\\
&-I_{0b}\ddot{u}_{0c}-I_{0b}\ddot{\phi}_{0c}\,h_c/2-I_{0b}\ddot{u}_{2c}\,h_c^2/4\\
&-I_{0b}\ddot{u}_{3c}\,h_c^3/8-I_{0b}\ddot{\phi}_b\,h_b/2-I_{1b}\ddot{\phi}_t\\
&-I_{0c}\ddot{u}_{0c}-I_{1c}\ddot{\phi}_{0c}-I_{2c}\ddot{u}_{2c}-I_{3c}\ddot{u}_{3c}\\
&-N^{t}_{xx,x}-N^{b}_{xx,x}-R^{c}_{x,x}=0
\end{aligned}
\tag{23}
$$

$$
\begin{aligned}
&+I_{0t}\ddot{u}_{0c}\,h_c/2-I_{0t}\ddot{\phi}_{0c}\,h_c^2/4+I_{0t}\ddot{u}_{2c}\,h_c^3/8\\
&-I_{0t}\ddot{u}_{3c}\,h_c^4/16-I_{0t}\ddot{\phi}_t\,h_t h_c/4+I_{1t}\ddot{\phi}_t\,h_c/2\\
&-I_{0b}\ddot{u}_{0c}\,h_c/2-I_{0b}\ddot{\phi}_{0c}\,h_c^2/4-I_{0b}\ddot{u}_{2c}\,h_c^3/8\\
&-I_{0b}\ddot{u}_{3c}\,h_c^4/16-I_{0b}\ddot{\phi}_b\,h_b h_c/4-I_{1b}\ddot{\phi}_b\,h_c/2\\
&-I_{1c}\ddot{u}_{0c}-I_{2c}\ddot{\phi}_{0c}-I_{3c}\ddot{u}_{2c}-I_{4c}\ddot{u}_{3c}+h_c/2N^{t}_{xx,x}\\
&-h_c/2N^{b}_{xx,x}-M^{c}_{x1,x}+Q^{c}_{xz}=0
\end{aligned}
\tag{24}
$$

$$
\begin{aligned}
&-I_{0t}\ddot{u}_{0c}\,h_c^2/4+I_{0t}\ddot{\phi}_{0c}\,h_c^3/8-I_{0t}\ddot{u}_{2c}\,h_c^4/16\\
&+I_{0t}\ddot{u}_{3c}\,h_c^5/32+I_{0t}\ddot{\phi}_t\,h_t h_c^2/8-I_{1t}\ddot{\phi}_t\,h_c^2/4\\
&-I_{0b}\ddot{u}_{0c}\,h_c^2/4-I_{0b}\ddot{\phi}_{0c}\,h_c^3/8-I_{0b}\ddot{u}_{2c}\,h_c^4/16\\
&-I_{0b}\ddot{u}_{3c}\,h_c^5/32-I_{0b}\ddot{\phi}_b\,h_b h_c^2/8\\
&-I_{1b}\ddot{\phi}_b\,h_c^2/4-I_{2c}\ddot{u}_{0c}-I_{3c}\ddot{\phi}_{0c}-I_{4c}\ddot{u}_{2c}\\
&-I_{5c}\ddot{u}_{3c}-h_c^2/4N^{t}_{xx,x}-h_c^2/4N^{b}_{xx,x}\\
&-M^{c}_{x2,x}+2M^{c}_{Q1xc}=0
\end{aligned}
\tag{25}
$$

$$
\begin{aligned}
&+I_{0t}\ddot{u}_{0c}\,h_c^3/8-I_{0t}\ddot{\phi}_{0c}\,h_c^4/16+I_{0t}\ddot{u}_{2c}\,h_c^5/32\\
&-I_{0t}\ddot{u}_{3c}\,h_c^6/64-I_{0t}\ddot{\phi}_t\,h_t h_c^3/16\\
&+I_{1t}\ddot{\phi}_t\,h_c^3/8-I_{0b}\ddot{u}_{0c}\,h_c^3/8-I_{0b}\ddot{\phi}_{0c}\,h_c^4/16\\
&-I_{0b}\ddot{u}_{2c}\,h_c^5/32-I_{0b}\ddot{u}_{3c}\,h_c^6/64\\
&-I_{0b}\ddot{\phi}_b\,h_b h_c^3/16-I_{1b}\ddot{\phi}_b\,h_c^3/8-I_{3c}\ddot{u}_{0c}-\\
&I_{4c}\ddot{\phi}_{0c}-I_{5c}\ddot{u}_{2c}-I_{6c}\ddot{u}_{3c}+h_c^3/8N^{t}_{xx,x}\\
&-h_c^3/8N^{b}_{xx,x}-M^{c}_{x3,x}+3M^{c}_{Q2xc}=0
\end{aligned}
\tag{26}
$$

$$
\begin{aligned}
&-I_{0t}\ddot{w}_{0c}+I_{0t}\ddot{w}_{1c}\,h_c/2-I_{0t}\ddot{w}_{2c}-I_{0b}\ddot{w}_{0c}\\
&-I_{0b}\ddot{w}_{1c}\,h_c/2-I_{0b}\ddot{w}_{2c}\,h_c^2/4-\\
&I_{0c}\ddot{w}_{0c}-I_{1c}\ddot{w}_{0c}-I_{2c}\ddot{w}_{2c}-N^{t}_{xz,x}-\\
&N^{b}_{xz,x}-Q^{c}_{xz,x}-N^{tT}_{xx,x}w_{0c,x}-N^{tT}_{xx}w_{0c,xx}+\\
&N^{tT}_{xx,x}w_{1c,x}\,h_c/2+N^{tT}_{xx}w_{1c,xx}\,h_c/2-\\
&N^{tT}_{xx,x}w_{2c,x}\,h_c^2/4-N^{tT}_{xx}w_{2c,xx}\,h_c^2/4-\\
&N^{bT}_{xx,x}w_{0c,x}-N^{bT}_{xx}w_{0c,xx}-N^{bT}_{xx,x}w_{1c,x}\,h_c/2\\
&-N^{bT}_{xx}w_{1c,xx}\,h_c/2-N^{bT}_{xx,x}w_{2c,x}\,h_c^2/4\\
&-N^{bT}_{xx}w_{2c,xx}\,h_c^2/4=0
\end{aligned}
\tag{27}
$$

$$
\begin{aligned}
&+I_{0t}\ddot{w}_{0c}\,h_c/2-I_{0t}\ddot{w}_{1c}\,h_c^2/4+I_{0t}\ddot{w}_{2c}\,h_c^3/8\\
&-I_{0b}\ddot{w}_{0c}\,h_c/2-I_{0b}\ddot{w}_{1c}\,h_c^2/4-\\
&I_{0b}\ddot{w}_{2c}\,h_c^3/8-I_{1c}\ddot{w}_{0c}-I_{2c}\ddot{w}_{0c}-I_{3c}\ddot{w}_{2c}\\
&+h_c/2N^{t}_{xz,x}-h_c/2N^{b}_{xz,x}-M^{c}_{Q1xc,x}\\
&+R^{c}_{z}-N^{tT}_{xx,x}w_{1c,x}\,h_c^2/4-N^{tT}_{xx}w_{1c,xx}\,h_c^2/4\\
&+N^{tT}_{xx,x}w_{0c,x}\,h_c/2+N^{tT}_{xx}w_{0c,xx}\,h_c/2+\\
&N^{tT}_{xx,x}w_{2c,x}\,h_c^3/8+N^{tT}_{xx}w_{2c,xx}\,h_c^3/8\\
&-N^{bT}_{xx,x}w_{1c,x}\,h_c^2/4-N^{bT}_{xx}w_{1c,xx}\,h_c^2/4-\\
&N^{bT}_{xx,x}w_{0c,x}\,h_c/2-N^{bT}_{xx}w_{0c,xx}\,h_c/2-\\
&N^{bT}_{xx,x}w_{2c,x}\,h_c^3/8-N^{bT}_{xx}w_{2c,xx}\,h_c^3/8=0
\end{aligned}
\tag{28}
$$

$$
\begin{aligned}
&-I_{0t}\ddot{w}_{0c}\,h_c^2/4+I_{0t}\ddot{w}_{1c}\,h_c^3/8-I_{0t}\ddot{w}_{2c}\,h_c^4/16\\
&-I_{0b}\ddot{w}_{0c}\,h_c^2/4-I_{0b}\ddot{w}_{1c}\,h_c^3/8\\
&-I_{0b}\ddot{w}_{2c}\,h_c^4/16-I_{2c}\ddot{w}_{0c}-I_{3c}\ddot{w}_{0c}\\
&-I_{4c}\ddot{w}_{2c}-h_c^2/4N^{t}_{xz,x}-h_c^2/4N^{b}_{xz,x}\\
&-M^{c}_{Q2xc,x}+2M^{c}_{z}-N^{tT}_{xx,x}w_{2c,x}\,h_c^4/16\\
&-N^{tT}_{xx}w_{2c,xx}\,h_c^4/16-N^{tT}_{xx,x}w_{0c,x}\,h_c^2/4-\\
&N^{tT}_{xx}w_{0c,xx}\,h_c^2/4+N^{tT}_{xx,x}w_{1c,x}\,h_c^3/8+\\
&N^{tT}_{xx}w_{1c,xx}\,h_c^3/8-N^{bT}_{xx,x}w_{2c,x}\,h_c^4/16-\\
&N^{bT}_{xx}w_{2c,xx}\,h_c^4/16-N^{bT}_{xx,x}w_{0c,x}\,h_c^2/4-\\
&N^{bT}_{xx}w_{0c,xx}\,h_c^2/4-N^{bT}_{xx,x}w_{1c,x}\,h_c^3/8-\\
&N^{bT}_{xx}w_{1c,xx}\,h_c^3/8=0
\end{aligned}
\tag{29}
$$

$$u_{0t}+\frac{h_t}{2}\phi^{t}=u_{0c}-\frac{h_c}{2}\phi_0^{c}+\frac{h_c^2}{4}u_{2c}-\frac{h_c^3}{8}u_{3c}=0 \tag{30}$$

$$w_{0t}=+w_{0c}-\mathrm{h_c}/2\,w_{1c}+\mathrm{h_c}^2/4\,w_{2c} \tag{31}$$

$$u_{0b}-\frac{h_b}{2}\phi^{b}=u_{0c}+\frac{h_c}{2}\phi_0^{c}+\frac{h_c^2}{4}u_{2c}+\frac{h_c^3}{8}u_{3c}=0 \tag{32}$$

$$w_{0b}=+w_{0c}+\mathrm{h_c}/2\,w_{1c}+\mathrm{h_c}^2/4\,w_{2c} \tag{33}$$

where "I_{kt}", "I_{kb}" (k=0, 1, 2) are the inertia terms of the top and the bottom face sheets, respectively; "I_{lc}" (l=0, 1,…,6) are the inertia terms of the core. "N^{j}_{xx}", "N^{j}_{xz}", (j=t, b) are the stress resultants and "M^{j}_{xx}" (j=t, b) are the moment resultants of the top and the bottom face sheets; "N^{jT}_{xx}", "N^{jT}_{zz}", (j=t,b) are the force thermal resultants; "Q_{xc}", "M_{Q1xc}", "M_{Q2xc}", "R_{zc}", "M_{zc}", "R_{xc}", "M_{x1c}", "M_{x2c}" and "M_{x3c}" are the high order stress resultant of the core. In the relations of the face sheets, the in-plane stress resultants, "N_{xx}"; the moment resultants, "M_{xx}"; and the out of plane

shear stress resultants, "N_{xz}", are calculated as follows [38]:

$$N_{xx}^{j} = A_{11}u_{0,x}^{j} + B_{11}\phi_{,x}^{j} - N_{xx}^{jT}\ , j = (t,b) \tag{34}$$

$$M_{xx}^{j} = B_{11}u_{0,x}^{j} + D_{11}\phi_{,x}^{j} - M_{xx}^{jT} \tag{35}$$

$$N_{xz}^{j} = \pi^2/12\, A_{44}(\phi^{j} + w_{0,x}^{j}) \tag{36}$$

"A" is the stretching stiffness, "B" is the bending-stretching stiffness and "D" is the bending stiffness; which are constant coefficients and express as [39]:

$$\begin{Bmatrix} A_{11}^{j} \\ B_{11}^{j} \\ D_{11}^{j} \end{Bmatrix} = \int_{-hj/2}^{hj/2} \left(\frac{E_j}{1-\nu_j^{\,2}} \right) \begin{Bmatrix} 1 \\ z_j \\ z_j^{\,2} \end{Bmatrix} dz_j$$
$$\{A_{44}^{j}\} = \int_{-hj/2}^{hj/2} \left(\frac{E_j}{2(1+\nu_j)} \right) dz_j \tag{37}$$

The high order thermal stress resultants in the face sheets are depicted as follows [39]:

$$\left\{N_{xx}^{jT}, N_{zz}^{jT}\right\} = -\int_{-hj/2}^{hj/2} \left(\frac{E_j}{1-\nu_j} \alpha_j T_j \right) d\, z_j\ , j = (t,b) \tag{38}$$

where "E", "ν" and "α" are the Young's modulus, the Poisson's ratio and the thermal expansion coefficient, respectively, which in the functionally graded layers are the function of the displacement, too. The inertia terms of the face sheets and the core are calculated as follows [38]:

$$\left(I_{0j}, I_{1j}, I_{2j}\right) = \int_{-hj/2}^{hj/2} \rho_j \left(1, z_j, z_j^{\,2}\right) dz_j\ , \quad \left(j = t,b\right) \tag{39}$$

$$\left(I_{0c}, I_{1c}, I_{2c}, I_{3c}, I_{4c}, I_{5c}, I_{6c}\right) = \int_{-hc/2}^{hc/2} \rho_c \left(1, z_c, z_c^{\,2}, z_c^{\,3}, z_c^{\,4}, z_c^{\,5}, z_c^{\,6}\right) dz_c \tag{40}$$

The high order stress resultants of the core are as follows:

$$Q_{xc}, M_{Q1xc}, M_{Q2xc} = \int_{-hc/2}^{hc/2} \left(1, z_c, z_c^{2}\right) \sigma_{xz}^{c} dz_c \tag{41}$$

$$R_{zc}, M_{zc} = \int_{-hc/2}^{hc/2} \left(1, z_c\right) \sigma_{zz}^{c} dz_c \tag{42}$$

$$R_x^c, M_{x1}^c, M_{x2}^c, M_{x3}^c = \int_{-hc/2}^{hc/2} \left(1, z_c, z_c^{2}, z_c^{3}\right) \sigma_{xx}^{c} dz_c \tag{43}$$

Finally, by substituting the high order stress resultants in terms of the kinematic relations, the equations are derived in terms of the nine unknowns.

3-Verification and numerical results

In order to solve the equations of the free vibration of the FG sandwich beam, a Galerkin method with nine trigonometric shape functions is established which satisfy the boundary condition. The shape functions of the clamped-free boundary condition can be expressed as [40]:

$$\phi_x^{j} = C_{\phi xj} \frac{\lambda_m}{L}\left(\sinh\left(\frac{\lambda_m x}{L}\right) + \sin\left(\frac{\lambda_m x}{L}\right) - \gamma_m\left(\cos h\left(\frac{\lambda_m x}{L}\right) - \cos\left(\frac{\lambda_m x}{L}\right)\right)\right) e^{i\omega t}\ , \quad j = (t,b) \tag{44}$$

$$u_{ck} = C_{uk} \frac{\lambda_m}{L}\left(\sinh\left(\frac{\lambda_m x}{L}\right) + \sin\left(\frac{\lambda_m x}{L}\right) - \gamma_m\left(\cos h\left(\frac{\lambda_m x}{L}\right) - \cos\left(\frac{\lambda_m x}{L}\right)\right)\right) e^{i\omega t} \tag{45}$$
$$,k = (0,1,2,3)$$

$$w_{ck} = C_{wk}\left(\cosh\left(\frac{\lambda_m x}{L}\right) - \cos\left(\frac{\lambda_m x}{L}\right) - \gamma_m\left(\sin h\left(\frac{\lambda_m x}{L}\right) - \sin\left(\frac{\lambda_m x}{L}\right)\right)\right) e^{i\omega t} \tag{46}$$
$$k = (0,1,2)$$

$$\cos\lambda_m . \cosh\lambda_m = -1$$
$$\lambda_m = 1.875, 4.694, 7.854, 10.995, 14.137 \tag{47}$$

$$\gamma_m = \frac{\sinh\lambda_m - \sin\lambda_m}{\cosh\lambda_m - \cos\lambda_m} \quad m = (1,2,3,...) \tag{48}$$

where "$a_m=m\pi/L$; "m" is the wave number and $C_{uk}, C_{wk}, C_{\phi j}$ are the nine unknown constants of the shape functions. These nine equations can be written in a 9×9 matrix which include the mass, "M", and stiffness, "K", matrices as follows:

$$(k_m - \omega_m^2 M_m) C_m = 0 \quad (49)$$

In Eq. (49), "ω_m" is the natural frequency; and "C_m" is the Eigen-vector which contains nine unknown constants.

In order to validate the approach of this study, present results in a special case are compared with results of literatures [41],[42], [43] which are shown in Table 1, for the simply supported (S-S) and clamped (C-C) boundary conditions.

Table 1. Fundamental frequency parameters of present results and literatures [41],[42], [43] (L/h=5)

B.C	reference	N=0	N=0.5	N=1	N=2
S-S	Simsek [41]	5.1525	4.4083	3.9902	3.6344
	Vo [43]	5.1526	4.3990	3.9711	3.6050
	Nguyen [42]	5.1525	4.4075	3.9902	3.6344
	Present method	5.0789	4.3312	3.8618	3.5487
C-C	Simsek [41]	10.0344	8.7005	7.9253	7.2113
	Vo [43]	9.9984	8.6717	7.9015	7.1901
	Present method	9.9151	8.5887	7.8080	7.1088

Consider a FG sandwich beam which is assumed to be made from a mixture of Silicon nitride as ceramic phase and Stainless steel as metal phase. The temperature-dependent properties of constituent materials which is introduced by Eq. (1) are presented in the reference [35]. For simplicity, the fundamental frequency parameter defined that is non-dimensional as:

$$\bar{\omega} = \omega / 1000 \quad (50)$$

In general, "h_t-h_c-h_b" sandwich beam is a structure with the indices of outer face sheet thickness, core thickness and inner face sheet thickness equal to "h_t", "h_c" and "h_b", respectively. Therefore, in 1-8-1 sandwich, the core thickness is eight times of the every face sheet thickness.

According to Eq. (1), temperature rising reduces the Young modulus of metal and ceramic. So, the strength of the materials reduces, which is an important reason in decreasing the frequency in high temperature conditions. Fig. 2 shows the fundamental frequency parameter variation versus the temperature for 1-8-1 FG face sheets sandwich beam with clamped-free boundary condition. Geometrical parameters are "h = 0.02m, L/h=5, m=1". By increasing the temperature, the fundamental frequency parameters decrease. As shown in Fig. 2, when N=0, the FG layers are made of full ceramic, as a result, the stability and resistant against the high temperature conditions are more than the other values of "N", so the fundamental frequency parameters of it are higher than others. By increasing the power law index, "N", the amount of the ceramic reduces in the structure which causes the young modulus of the FGM and the stability of the structures decrease. When "N=0", by increasing the temperature, the fundamental frequency parameter decreases 31.30%, for "N=1" and "N=2" it decreases 40.34%, and 43.25%, respectively.

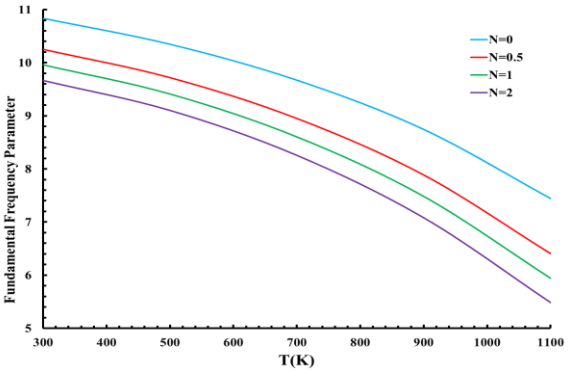

Fig. 2 Fundamental frequency variation versus temperature

Some geometrical effects on the fundamental frequency of FG sandwich beams are investigated. Figure 3 shows the effect of length to thickness ratio on the fundamental frequency parameter in 1-8-1 FG face sheets sandwich beam in the clamped-free boundary conditions. When ratios are increased in a constant "N", the fundamental frequency parameter decreases. Based on the Fig. 3, with increasing of this ratio, the stability of the structure is reduced and it is important to consider that long length is not proper for the FG sandwich beams. Also, it is obvious that, with increasing the power law index, "N", the fundamental frequency parameters decrease, but in this case effect of variation of the length is dominant parameter and its variation has an impressive effect on the fundamental frequency. For example, for L/h=5, by increasing "N", the fundamental frequency parameter decrease 10.80%, but for "N=0", by increasing this ratio, the fundamental frequency decreases 6130%. Also, it should be noted that when the ratio is more than 12, the slope of the variation of the fundamental frequency is decreased significantly.

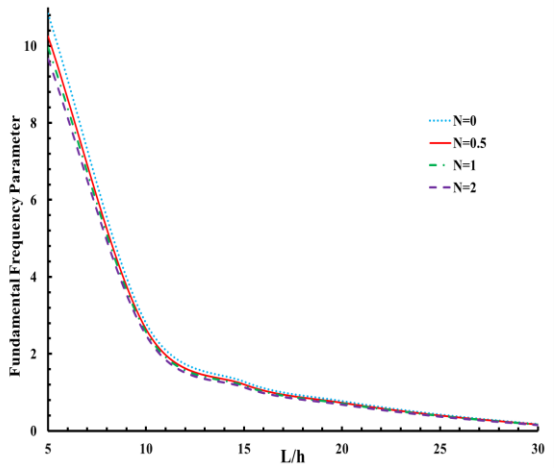

Fig. 3 Fundamental frequency variation versus L/h ratio

Fig. 4 depict the effect of the variation of the core to face sheet thickness ratio, "h_c/h_t", on the fundamental frequency parameter in various power law indices and constant total thickness. When "h_c/h_t=0.5", it means the thickness of the faces are two times of the core thickness, so it shows the results of the 2-1-2 sandwich. And, when "h_c/h_t=8", it shows results of the 1-8-1 sandwich. For all power law indices, by increasing the ratio in the constant total thickness, the amount of metal increases and the structure will be softer, so the fundamental frequency parameters decrease. Also, when the power law index is increased in a constant thickness, ceramic quantity will decrease and the fundamental frequency parameters decrease. For example, in "h_c/h_t=0.5", the fundamental frequency parameter decrease 32.62% when "N" is increased, and in "h_c/h_t=8", the fundamental frequency parameter decrease 11.06% when "N" is increased. Also, for "N=0", by increasing this ratio, the fundamental frequency decreases 36.47%.

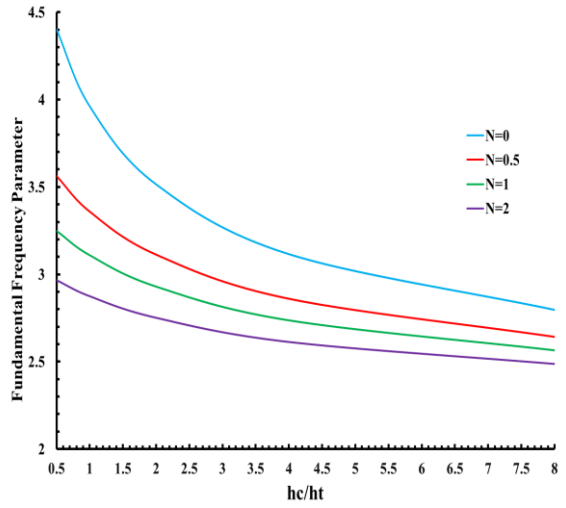

Fig. 4 Effect of variation of the core to face sheets thickness ratio on the fundamental frequency parameter

Effect of the variation of the wave number, "m", on the fundamental frequency parameter in various power law indices and constant total thickness is depicted in the Fig. 5. By increasing the wave number, the fundamental frequency parameters increase.

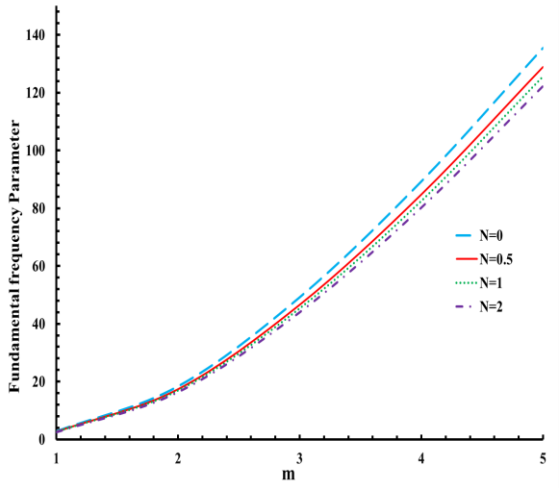

Fig. 5 Effect of variation of the wave number on the fundamental frequency parameter

Effect of the variation of the total thickness of the sandwiches, "h", on the fundamental frequency parameter in various power law indices for clamped-free FG sandwich beam is depicted in Fig. 5. It is obvious that by increasing the total thickness, the fundamental frequency parameter decreases. For example, in "N=0" by increasing the "h", the fundamental frequency parameter decrease 2462.63%. But, it is seen that after the "h=0.02m", the rate of variation is decreased and the differences is 561.48%. For "h=0.01m", by increasing "N", the fundamental frequency parameter decrease 10.80%.

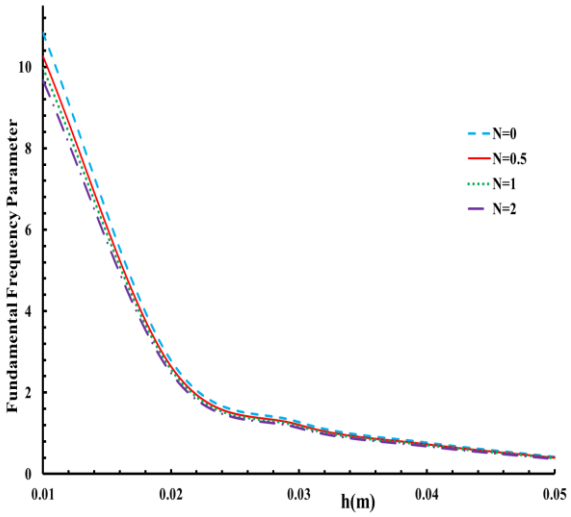

Fig. 6 Effect of the variation of the total thickness of the sandwiches on the fundamental frequency parameter

In order to investigate the porosity influence, Figs. 7 and 8 show the effect of even and uneven porosity distributions on the fundamental frequency parameters of sandwich beam, respectively. Geometrical parameters are "h = 0.02m, L/h=5, m=1". In even distributions, porosities occur all over the cross-section of FG layer. While, in uneven distribution, porosities are available at middle zone of cross section. As shown in Figs. 7 and 8, by increasing the porosity volume fraction, the fundamental frequency parameters decrease for all power law indices. the slope of decreasing are stronger in the case of even porosity distribution. In the even case in "N=0", by increasing the volume fraction of the porosity, the fundamental frequency decreases 10.82%, and in the uneven case in "N=0", by increasing the

volume fraction of the porosity, the fundamental frequency decreases 5.21%

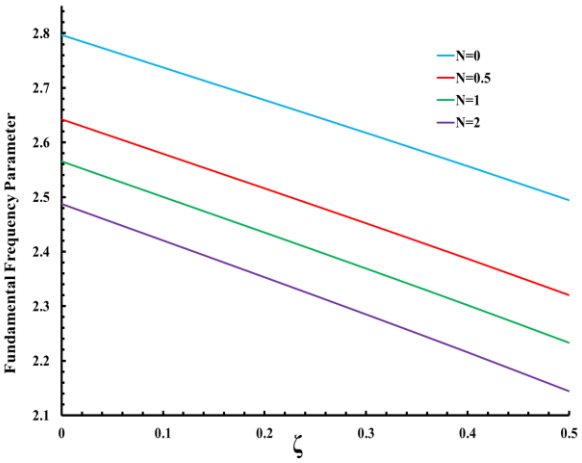

Fig. 7 Fundamental frequency variation versus even porosity.

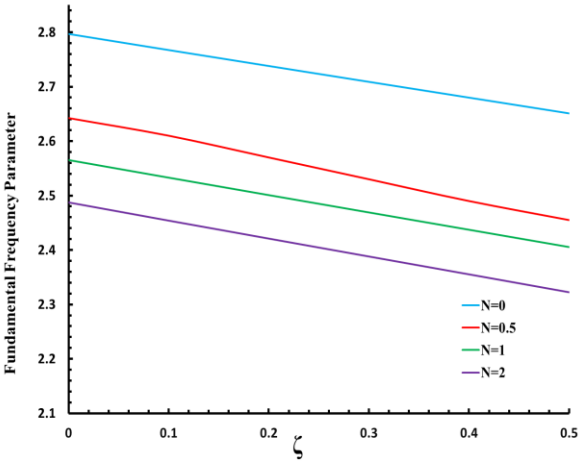

Fig. 8 Fundamental frequency variation versus uneven porosity

4-Conclusion

In this study, frequency analysis of 1-8-1 sandwich beams, according to a high order sandwich beam theory was presented. The displacement fields of the face-sheets were considered based on the first order shear deformation theory and the core displacement fields were considered as the polynomial distributions for vertical and horizontal deflections. High order stress resultants and in-plane stresses in the core and thermal stress resultants, and nonlinear strains in the face sheets were considered. All materials were temperature dependent. A power law distribution was used to model the material properties of the FG face sheets which modified by considering two distributions of porosity. The equations of motion were obtained by Hamilton's principal and solved by using Galerkin method for clamped-free boundary condition. In order to survey the capabilities of this model for free vibration analysis, the results were verified by literature results in a special case. Based on the results, there was a good agreement between them. The following conclusion can be drawn:

1. By increasing the temperature, the fundamental frequency parameters decrease.
2. While power law index is increased, the amount of ceramic reduces, so the fundamental frequency parameter decreases.
3. By increasing the length to thickness ratio, the stability of the structure reduces, so the fundamental frequency parameter decreased.
4. In a constant total thickness, with increasing the core to face-sheet thickness ratio in different power law indices, the fundamental frequency parameters decrease. For example, in the value of “hc/ht=0.5”, 2-1-2 type, FG faces sandwiches due to the more quantity of ceramic have stiffer structure than the value of “hc/ht=8”, 1-8-1 type, so the fundamental frequency parameter in 2-1-2 type is higher.
5. By increasing the wave number, the fundamental frequency parameter increases.
6. By increasing the total thickness of the sandwich beams, the fundamental frequency parameter decreases.

7. By increasing the porosity volume fraction in both even and uneven distributions, the fundamental frequency parameter decrease. Also, variation of frequencies in even porosity case is more than uneven case.

References

[1] Vinson, J. (2018). *The behavior of sandwich structures of isotropic and composite materials*: Routledge.

[2] Rahmani, M., Mohammadi, Y., & Kakavand, F. (2019). Vibration analysis of sandwich truncated conical shells with porous FG face sheets in various thermal surroundings. *Steel and Composite Structures, 32*(2), 239-252.

[3] Frostig, Y., Baruch, M., Vilnay, O., & Sheinman, I. (1992). High-order theory for sandwich-beam behavior with transversely flexible core. *Journal of Engineering Mechanics, 118*(5), 1026-1043.

[4] Fazzolari, F. A. (2018). Generalized exponential, polynomial and trigonometric theories for vibration and stability analysis of porous FG sandwich beams resting on elastic foundations. *Composites Part B: Engineering, 136*, 254-271.

[5] Chen, D., Kitipornchai, S., & Yang, J. (2016). Nonlinear free vibration of shear deformable sandwich beam with a functionally graded porous core. *Thin-Walled Structures, 107*, 39-48.

[6] Akbaş, Ş. D. (2017). Thermal effects on the vibration of functionally graded deep beams with porosity. *International Journal of Applied Mechanics, 9*(05), 1750076.

[7] Bourada, F., Bousahla, A. A., Bourada, M., Azzaz, A., Zinata, A., & Tounsi, A. (2019). Dynamic investigation of porous functionally graded beam using a sinusoidal shear deformation theory. *Wind and Structures, 28*(1), 19-30.

[8] Li, C., Shen, H.-S., & Wang, H. (2019). Nonlinear vibration of sandwich beams with functionally graded negative Poisson's ratio honeycomb core. *International Journal of Structural Stability and Dynamics, 19*(03), 1950034.

[9] Wu, H., Kitipornchai, S., & Yang, J. (2015). Free vibration and buckling analysis of sandwich beams with functionally graded carbon nanotube-reinforced composite face sheets. *International Journal of Structural Stability and Dynamics, 15*(07), 1540011.

[10] Xu, G.-d., Zeng, T., Cheng, S., Wang, X.-h., & Zhang, K. (2019). Free vibration of composite sandwich beam with graded corrugated lattice core. *Composite Structures, 229*, 111466.

[11] Li, M., Du, S., Li, F., & Jing, X. (2020). Vibration characteristics of novel multilayer sandwich beams: Modelling, analysis and experimental validations. *Mechanical Systems and Signal Processing, 142*, 106799.

[12] Li, Y., Dong, Y., Qin, Y., & Lv, H. (2018). Nonlinear forced vibration and stability of an axially moving viscoelastic sandwich beam. *International Journal of Mechanical Sciences, 138*, 131-145.

[13] Şimşek, M., & Al-Shujairi, M. (2017). Static, free and forced vibration of functionally graded (FG) sandwich beams excited by two successive moving harmonic loads. *Composites Part B: Engineering, 108*, 18-34.

[14] Nguyen, T.-K., Vo, T. P., Nguyen, B.-D., & Lee, J. (2016). An analytical solution for buckling and vibration analysis of functionally graded sandwich beams using a quasi-3D shear deformation theory. *Composite Structures, 156*, 238-252.

[15] Kahya, V., & Turan, M. (2018). Vibration and stability analysis of functionally graded sandwich beams by a multi-layer finite element. *Composites Part B: Engineering, 146*, 198-212.

[16] Tossapanon, P., & Wattanasakulpong, N. (2016). Stability and free vibration of functionally graded sandwich beams resting on two-parameter elastic foundation. *Composite Structures, 142*, 215-225.

[17] Amirani, M. C., Khalili, S., & Nemati, N. (2009). Free vibration analysis of sandwich beam with FG core using the element free Galerkin method. *Composite Structures, 90*(3), 373-379.

[18] Pradhan, S., & Murmu, T. (2009). Thermo-mechanical vibration of FGM sandwich beam under variable elastic foundations using differential quadrature method. *Journal of Sound and Vibration, 321*(1-2), 342-362.

[19] Mashat, D. S., Carrera, E., Zenkour, A. M., Al Khateeb, S. A., & Filippi, M. (2014). Free vibration of FGM layered

beams by various theories and finite elements. *Composites Part B: Engineering, 59*, 269-278.

[20] Nguyen, T.-K., Nguyen, T. T.-P., Vo, T. P., & Thai, H.-T. (2015). Vibration and buckling analysis of functionally graded sandwich beams by a new higher-order shear deformation theory. *Composites Part B: Engineering, 76*, 273-285.

[21] Vo, T. P., Thai, H.-T., Nguyen, T.-K., Inam, F., & Lee, J. (2015). A quasi-3D theory for vibration and buckling of functionally graded sandwich beams. *Composite Structures, 119*, 1-12.

[22] Yang, Y., Lam, C., Kou, K., & Iu, V. (2014). Free vibration analysis of the functionally graded sandwich beams by a meshfree boundary-domain integral equation method. *Composite Structures, 117*, 32-39.

[23] Abdolahi, I., & Yas, M. (2014). Vibration Analysis of Timoshenko Beam Reinforced With Boron-Nitride Nanotube on Elastic Bed. *Journal of Simulation and Analysis of Novel Technologies in Mechanical Engineering, 7*(3), 1-12.

[24] Farahani, H., Barati, F., Nejati, M., & Batmani, H. (2013). Vibration Analysis of Thick Functionally Graded Beam under Axial Load Based on Two-Dimensional Elasticity Theory and Generalized Differential Quadrature. *Journal of Simulation and Analysis of Novel Technologies in Mechanical Engineering, 6*(2), 59-71.

[25] Pirmoradian, M., & Karimpour, H. (2017). Parametric resonance and jump analysis of a beam subjected to periodic mass transition. *Nonlinear Dynamics, 89*(3), 2141-2154.

[26] Pirmoradian, M., Torkan, E., & Toghraie, D. (2020). Study on size-dependent vibration and stability of DWCNTs subjected to moving nanoparticles and embedded on two-parameter foundations. *Mechanics of Materials, 142*, 103279.

[27] Pirmoradian, M., Torkan, E., Zali, H., Hashemian, M., & Toghraie, D. (2020). Statistical and parametric instability analysis for delivery of nanoparticles through embedded DWCNT. *Physica A: Statistical Mechanics and Its Applications, 554*, 123911.

[28] Torkan, E., Pirmoradian, M., & Hashemian, M. (2017). Occurrence of parametric resonance in vibrations of rectangular plates resting on elastic foundation under passage of continuous series of moving masses. *Modares Mechanical Engineering, 17*(9), 225-236.

[29] Torkan, E., Pirmoradian, M., & Hashemian, M. (2019). Dynamic instability analysis of moderately thick rectangular plates influenced by an orbiting mass based on the first-order shear deformation theory. *Modares Mechanical Engineering, 19*(9), 2203-2213.

[30] Torkan, E., & Pirmoradian, M. (2019). Efficient higher-order shear deformation theories for instability analysis of plates carrying a mass moving on an elliptical path. *Journal of Solid Mechanics, 11*(4), 790-808.

[31] Heydari, E., Mokhtarian, A., Pirmoradian, M., Hashemian, M., & Seifzadeh, A. (2020). Sound transmission loss of a porous heterogeneous cylindrical nanoshell employing nonlocal strain gradient and first-order shear deformation assumptions. *Mechanics Based Design of Structures and Machines*, 1-22.

[32] Heydari, E., Mokhtarian, A., Pirmoradian, M., Hashemian, M., & Seifzadeh, A. (2021). Acoustic wave transmission of double-walled functionally graded cylindrical microshells under linear and nonlinear temperature distributions using modified strain gradient theory. *Thin-Walled Structures, 169*, 108430.

[33] Mohammadi, Y., H Safari, K., & Rahmani, M. (2016). Free vibration analysis of circular sandwich plates with clamped FG face sheets. *Journal of Simulation and Analysis of Novel Technologies in Mechanical Engineering, 9*(4), 631-646.

[34] Rahmani, M., Mohammadi, Y., Kakavand, F., & Raeisifard, H. (2020). Vibration analysis of different types of porous FG conical sandwich shells in various thermal surroundings. *Journal of Applied and Computational Mechanics, 6*(3), 416-432.

[35] Reddy, J. N. (2003). *Mechanics of laminated composite plates and shells: theory and analysis*: CRC press.

[36] Dariushi, S., & Sadighi, M. (2014). A new nonlinear high order theory for sandwich beams: An analytical and experimental

investigation. *Composite Structures, 108*, 779-788.
[37] Rahmani, M., Mohammadi, Y., & Kakavand, F. (2020). Buckling analysis of different types of porous fg conical sandwich shells in various thermal surroundings. *Journal of the Brazilian Society of Mechanical Sciences and Engineering, 42*(4), 1-16.
[38] Rahmani, M., & Dehghanpour, S. (2021). Temperature-Dependent Vibration of Various Types of Sandwich Beams with Porous FGM Layers. *International Journal of Structural Stability and Dynamics, 21*(02), 2150016.
[39] Mohammadi, Y., & Rahmani, M. (2020). Temperature-dependent buckling analysis of functionally graded sandwich cylinders. *Journal of Solid Mechanics, 12*(1), 1-15.
[40] Rahmani, M., & Mohammadi, Y. (2021). Vibration of two types of porous FG sandwich conical shell with different boundary conditions. *Structural Engineering and Mechanics, 79*(4), 401-413.
[41] Şimşek, M. (2010). Fundamental frequency analysis of functionally graded beams by using different higher-order beam theories. *Nuclear Engineering and Design, 240*(4), 697-705.
[42] Nguyen, T.-K., Vo, T. P., & Thai, H.-T. (2013). Static and free vibration of axially loaded functionally graded beams based on the first-order shear deformation theory. *Composites Part B: Engineering, 55*, 147-157.
[43] Vo, T. P., Thai, H.-T., Nguyen, T.-K., Maheri, A., & Lee, J. (2014). Finite element model for vibration and buckling of functionally graded sandwich beams based on a refined shear deformation theory. *Engineering Structures, 64*, 12-22.